Supplementary Information

Characterizing a Nitrogen Microwave Inductively Coupled Atmospheric-Pressure Plasma Ion Source for Element Mass Spectrometry

Monique Kuonen, Guanghui Niu, Bodo Hattendorf* and Detlef Günther
*Correspondence: Bodo Hattendorf, E-mail: bodo@inorg.chem.ethz.ch, Laboratory of Inorganic Chemistry, Department of Chemistry and Applied Biosciences, ETH Zurich, Vladimir – Prelog – Weg 1, 8093 Zurich, Switzerland

The following supplementary information supports the corresponding paper with additional figures (Figure S1 – S12) and a more detailed figure of merits table (Table S1), while also serving as an overview of the sensitivity contour plots of all measured elements for the different employed interface modifications (Figure S12 – S33). All Figures depicting signal intensities and abundance normalized sensitivities (Figure S3 – Figure S33) were obtained by measuring each m/z value with a dwell time of 500 ms and five replicates. The error bars representing two times the standard deviation are indicated but are hardly visible in such representations.

List of Figures

List of Tables

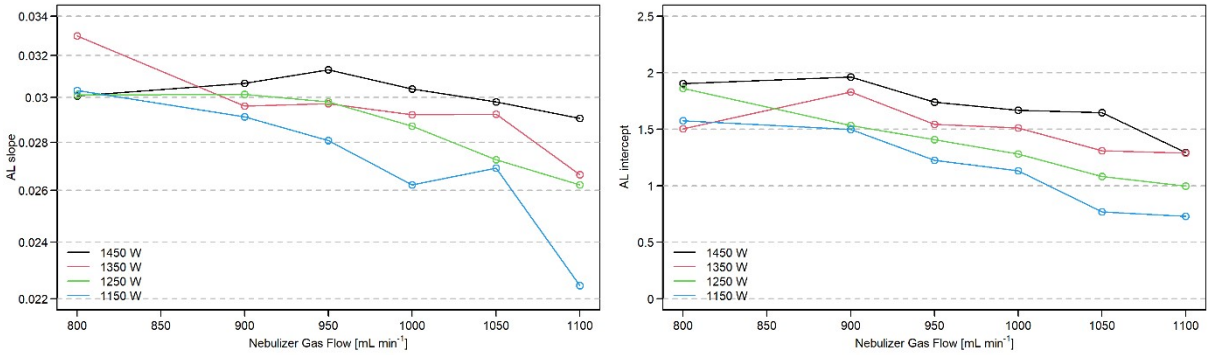

Figure S1: The dependence of the slope (left) and the intercept (right) of the ion lens voltage calibration curves on the nebulizer gas flow rate with the standard interface configuration. Each colour represents a measurement series with a fixed forward power. The value at 850 mL min^{-1} was not measured.

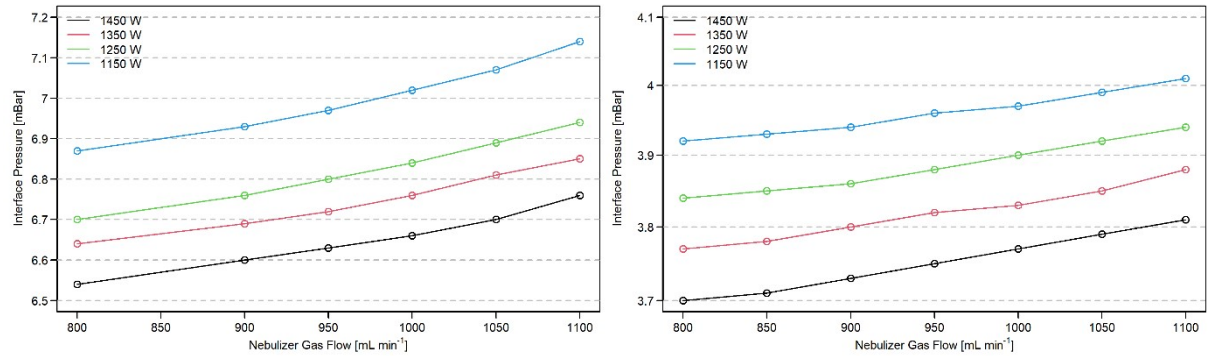

Figure S2: The measured interface pressure of the standard interface configuration is shown on the left, while the interface pressure is given on the right for the standard interface & pump configuration. The dependence of the nebulizer gas flow rate differs for the configurations in which each colour represents a measurement series with a fixed forward power.

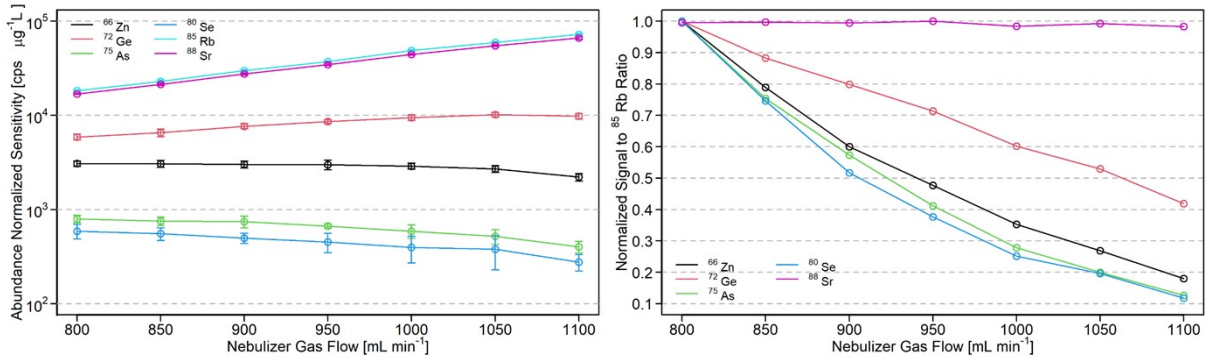

Figure S3: The abundance normalized sensitivity of elements with similar mass and different first ionization energies is shown on the left, while the ion loss in dependence of the nebulizer gas flow rate is depicted on the right by normalizing the analyte ^{85}Rb ratio to its maximum. Measurements were performed at 1350 W with the standard interface & pump configuration.

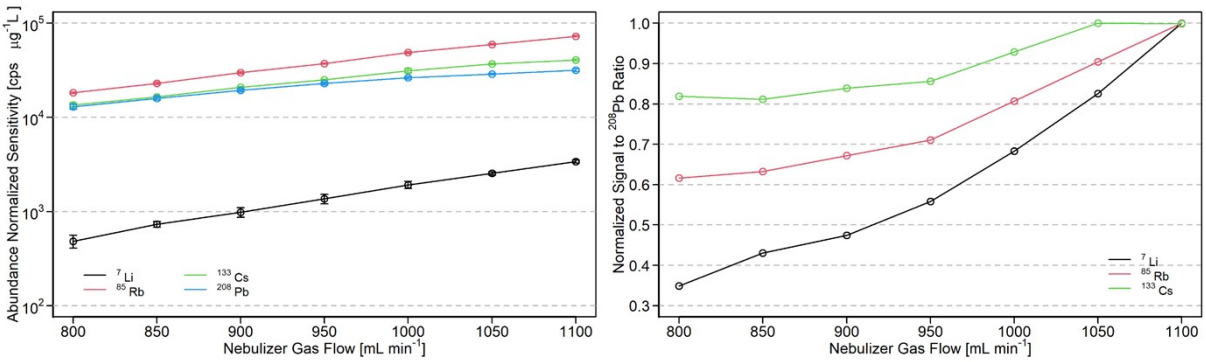

Figure S4: The abundance normalized sensitivities of some alkali elements and ^{208}Pb are shown on the left. ^{23}Na and ^{39}K are excluded due to contamination. On the right, the dependence of the sensitivity on the nebulizer gas flow is normalized to the maximal signal for Pb. Measurements were performed at 1350 W with the standard interface and the second interface pump.

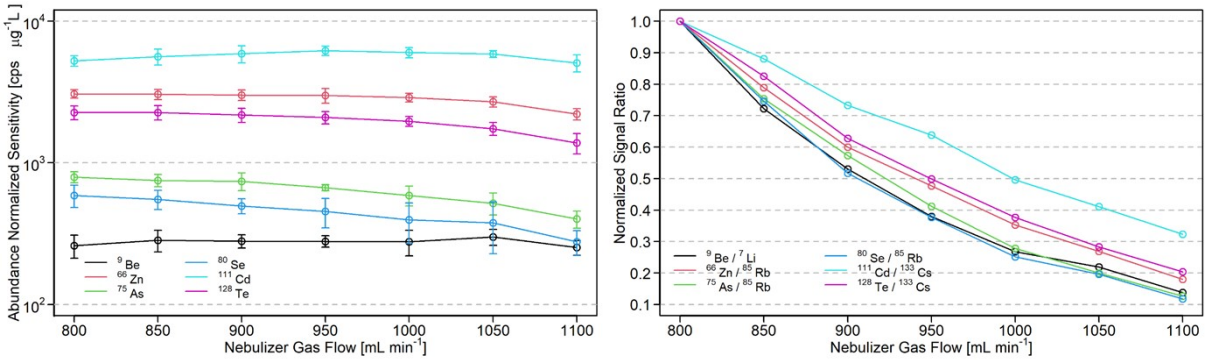

Figure S5: The abundance normalized sensitivity of elements with first ionization energies of about 9 eV or higher and different m/z are shown on the left. The relative suppression in dependence of the nebulizer gas flow is depicted on the right by the intensity ratio of the analyte to an analyte with similar m/z and a low ionization energy. The intensity ratio is normalized to its maximum. Measurements performed at 1350 W with the standard interface & pump configuration.

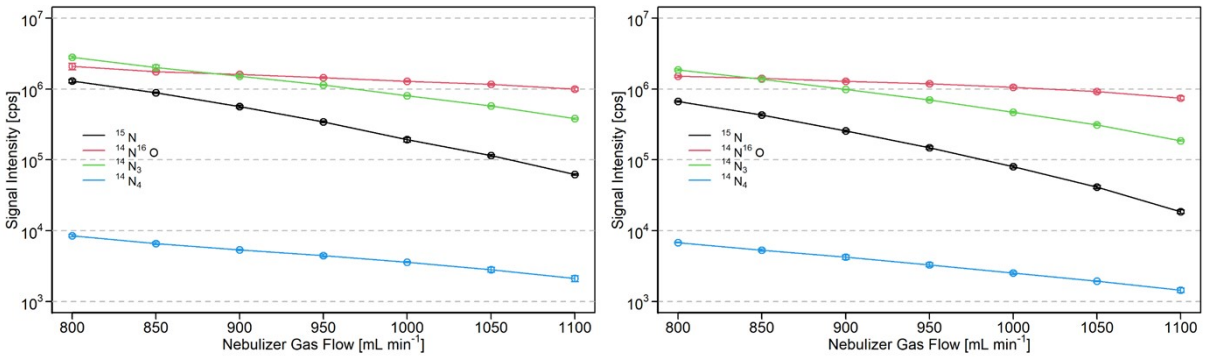

Figure S6: The measured plasma background ions are given in counts per second for the configuration with the standard interface and the second interface pump with their dependence on the nebulizer gas flow rate. On the left, the ions were measured at 1450 W and on the right at 1350 W. Please note, that $^{14}N^{16}O^+$ ion signals were attenuated by approximately 3 orders of magnitude by increasing the mass resolution to lower the signal intensity and avoid damaging the detector.

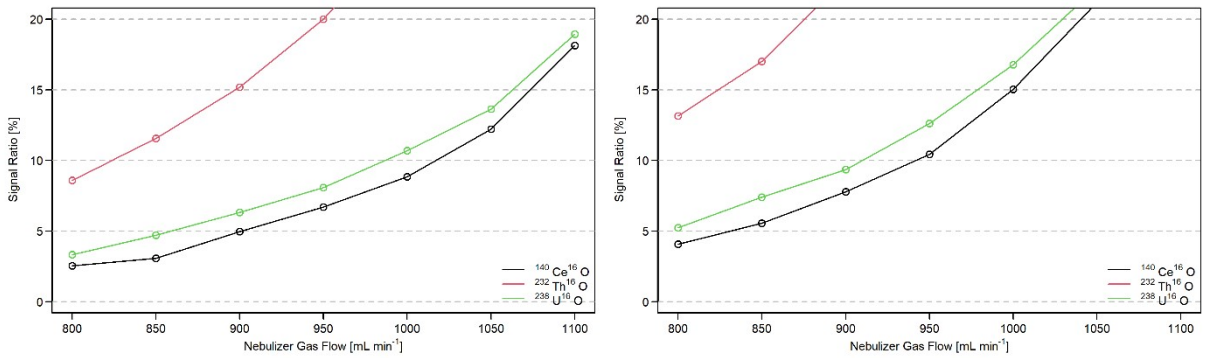

Figure S7: The dependence of the calculated oxide ratios on the nebulizer gas flow rate for the configuration with the standard interface and the second interface pump is shown on the left with a forward power of 1450 W and on the right with 1350 W.

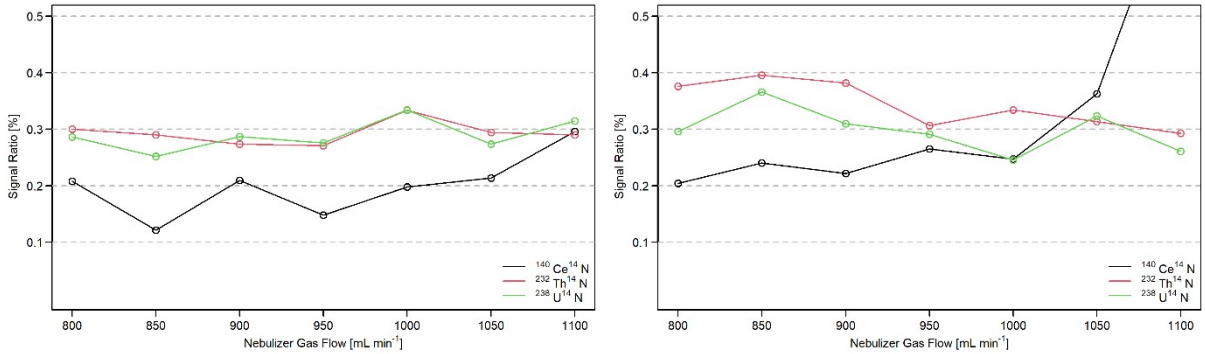

Figure S8: The dependence of the calculated nitride ratios on the nebulizer gas flow rate for the configuration with the standard interface and the second interface pump is shown on the left with a forward power of 1450 W and on the right with 1250 W.

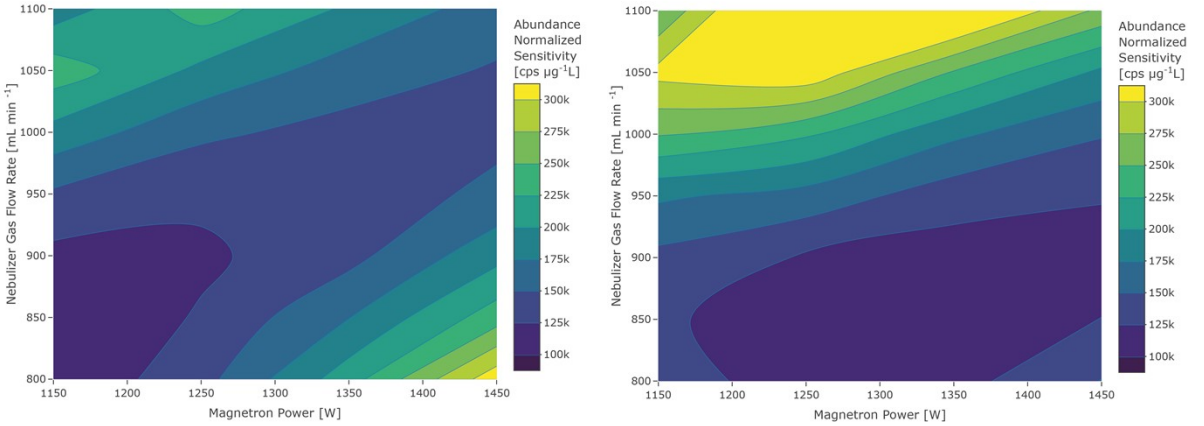

Figure S9: The bimodal behaviour of the ^{40}Ca contour plot seen for the standard interface and pump configuration (left) is not observed with the use of a reduced sampler orifice (right). Only the peak corresponding to a low forward power and a high gas flow remains.

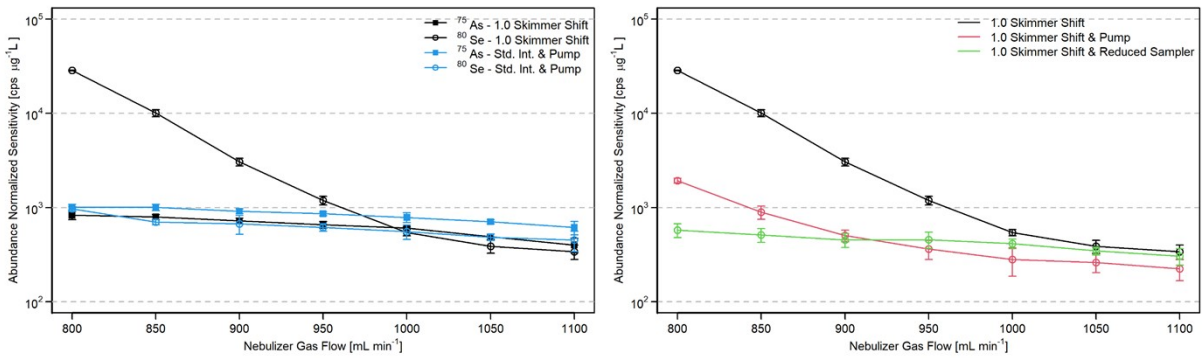

Figure S10: The trends of $^{75}As^{+}$ and $^{80}Se^{+}$ are shown on the left for the standard interface & pump, which do not show increased ion signals and with skimmer shift, causing the elevation at m/z 80. The right figure shows different configurations, where the elevation appeared at different magnitudes. Since the difference only occurred at a forward power of 1450 W, both plots stem from measurement series at 1450 W.

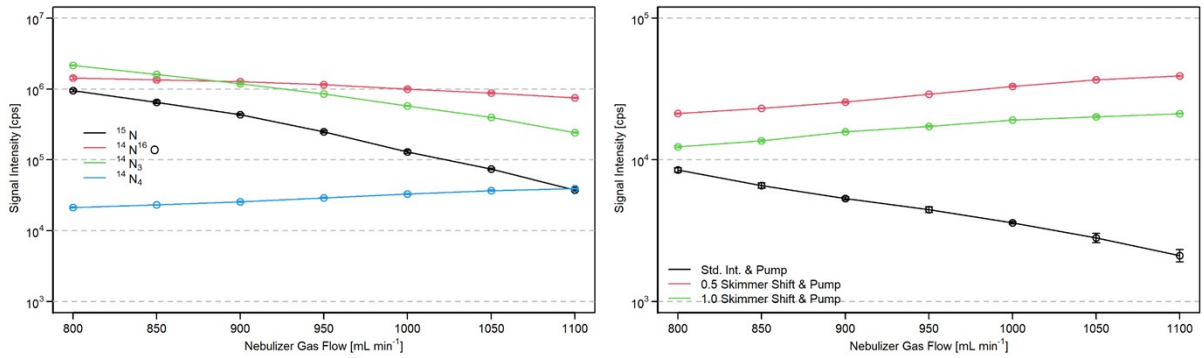

Figure S11: The plasma background ion trends measured at a forward power of 1450 W of the configuration with a 0.5 mm skimmer shift and the second interface pump given on the left show an increase in the abundance of $^{14}N_4$ with increasing nebulizer gas flow. This is contrary to the trend seen in other configurations as can be seen on the right, in which interface configurations with the second interface pump and with or without a skimmer position shift are compared at a forward power of 1450 W.

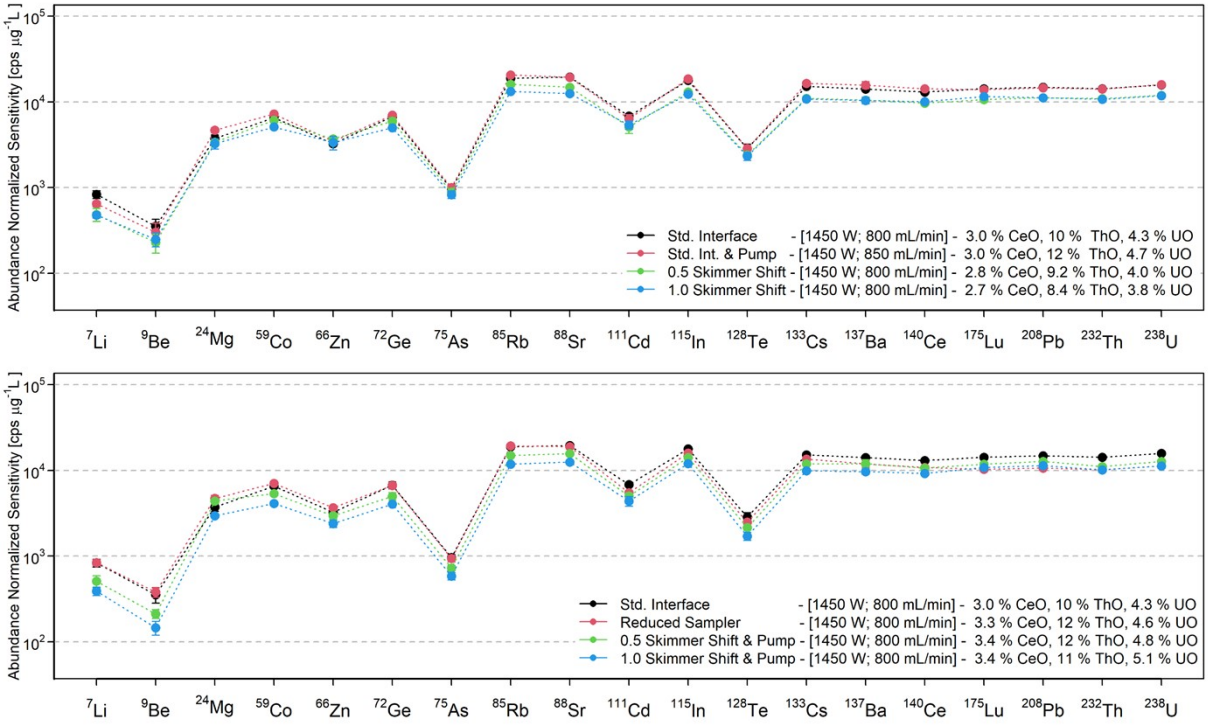

Figure S12: The response curves of seven different interface configurations are shown with their operating conditions and their oxide ratios. The configurations which achieve CeO^+ ratios of 3 % or lower are shown on the top, while those configurations with a ratio higher than 3 % are given on the bottom. The standard interface is depicted in both to facilitate the comparison. ^{80}Se is excluded in the comparison due to its different trend in some interface configurations. (All lines are to guide the eye.)

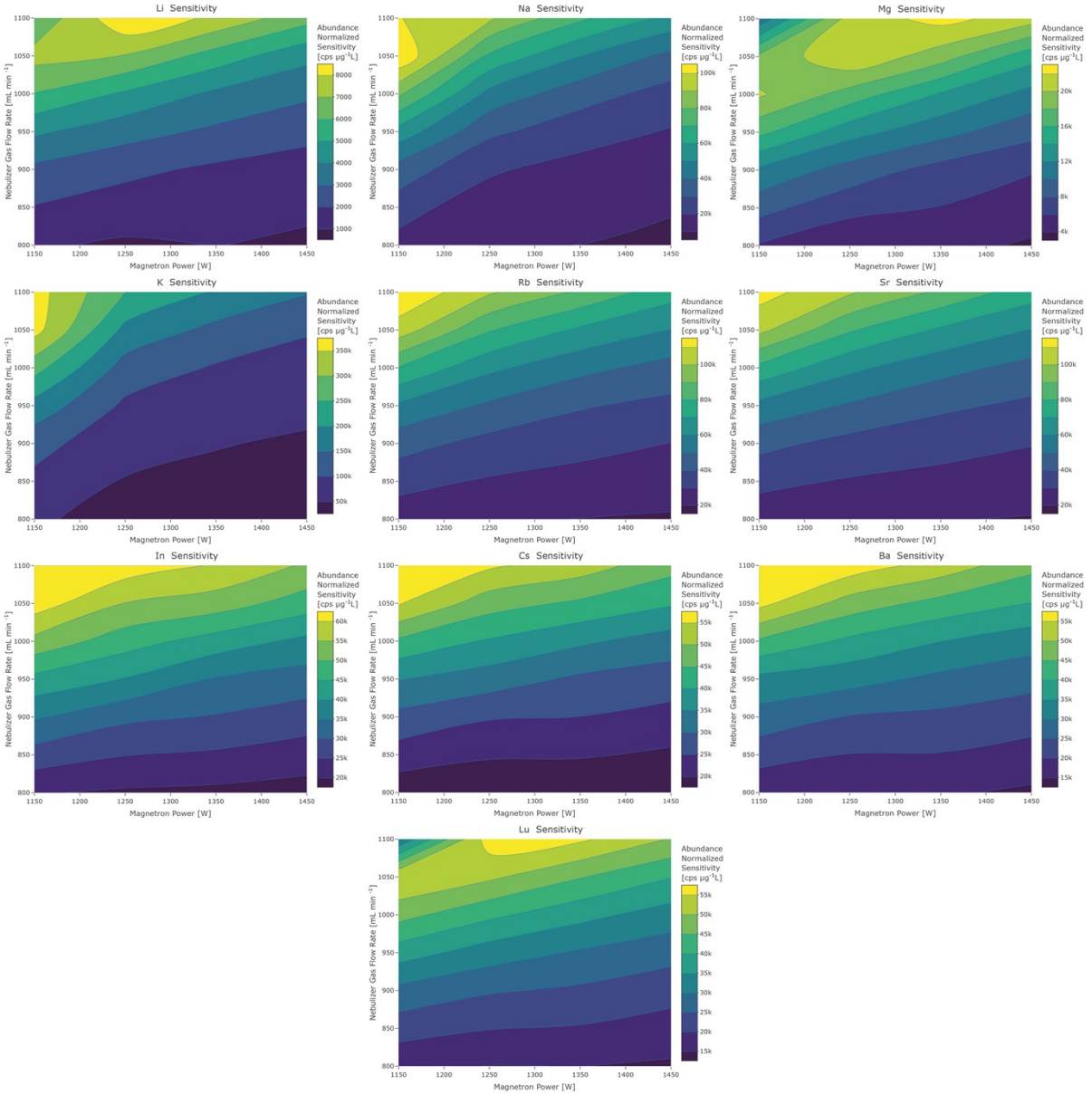

Figure S13: Sensitivity contour plots for the analytes ^{7}Li, ^{23}Na, ^{24}Mg, ^{39}K, ^{85}Rb, ^{88}Sr, ^{115}In, ^{133}Cs, ^{137}Ba and ^{175}Lu that belong to the first group, measured with the standard interface.

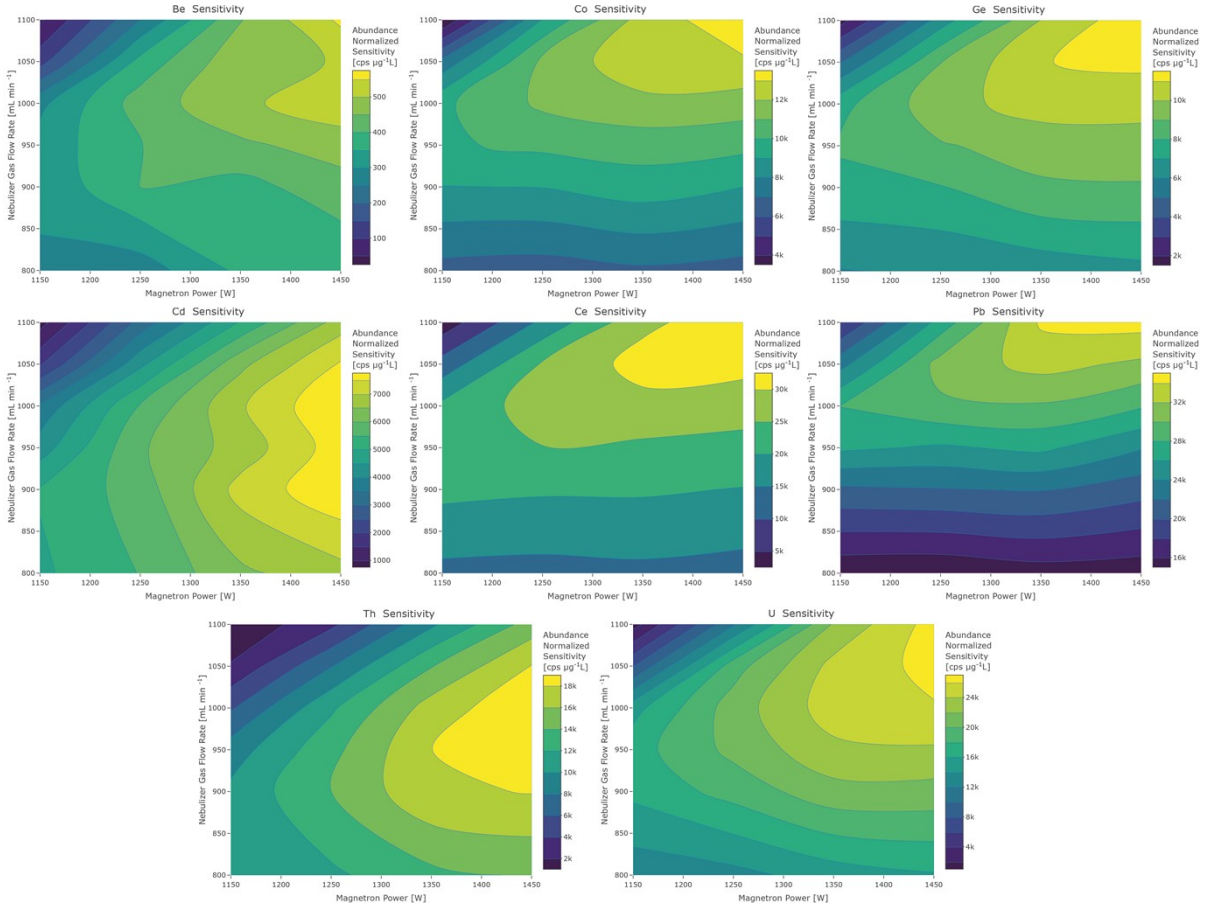

Figure S14: Sensitivity contour plots for the analytes ^{9}Be, ^{59}Co, ^{72}Ge, ^{111}Cd, ^{140}Ce, ^{208}Pb, ^{232}Th and ^{238}U that belong to the second group, measured with the standard interface.

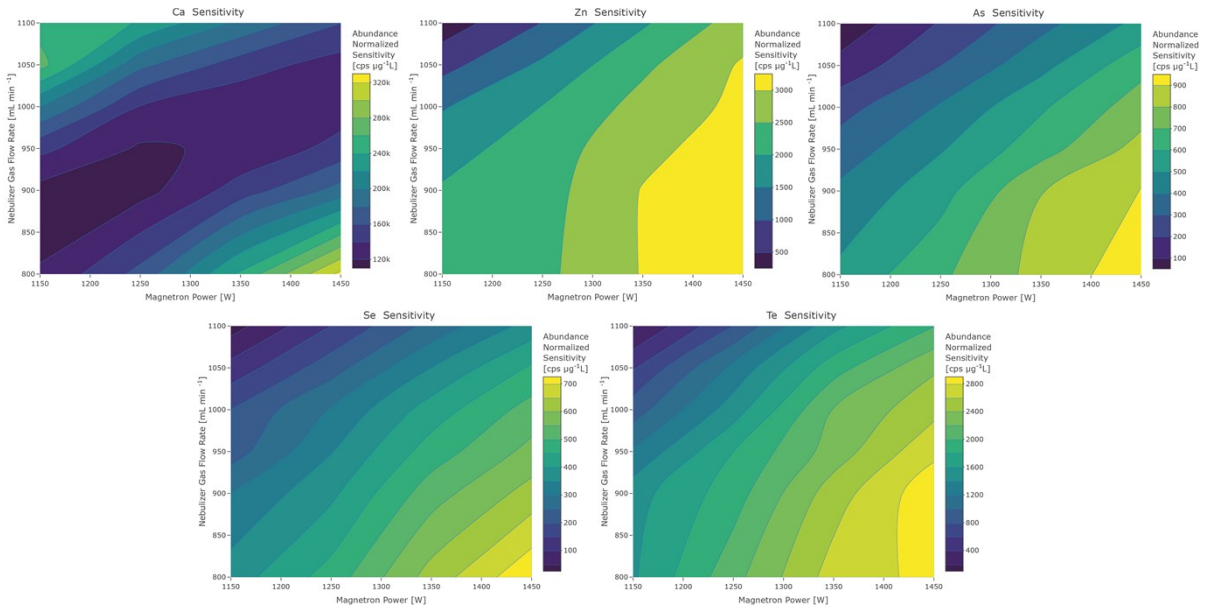

Figure S15: Sensitivity contour plots for the analytes ^{40}Ca, ^{66}Zn, ^{75}As, ^{80}Se and ^{128}Te that belong to the third group, measured with the standard interface.

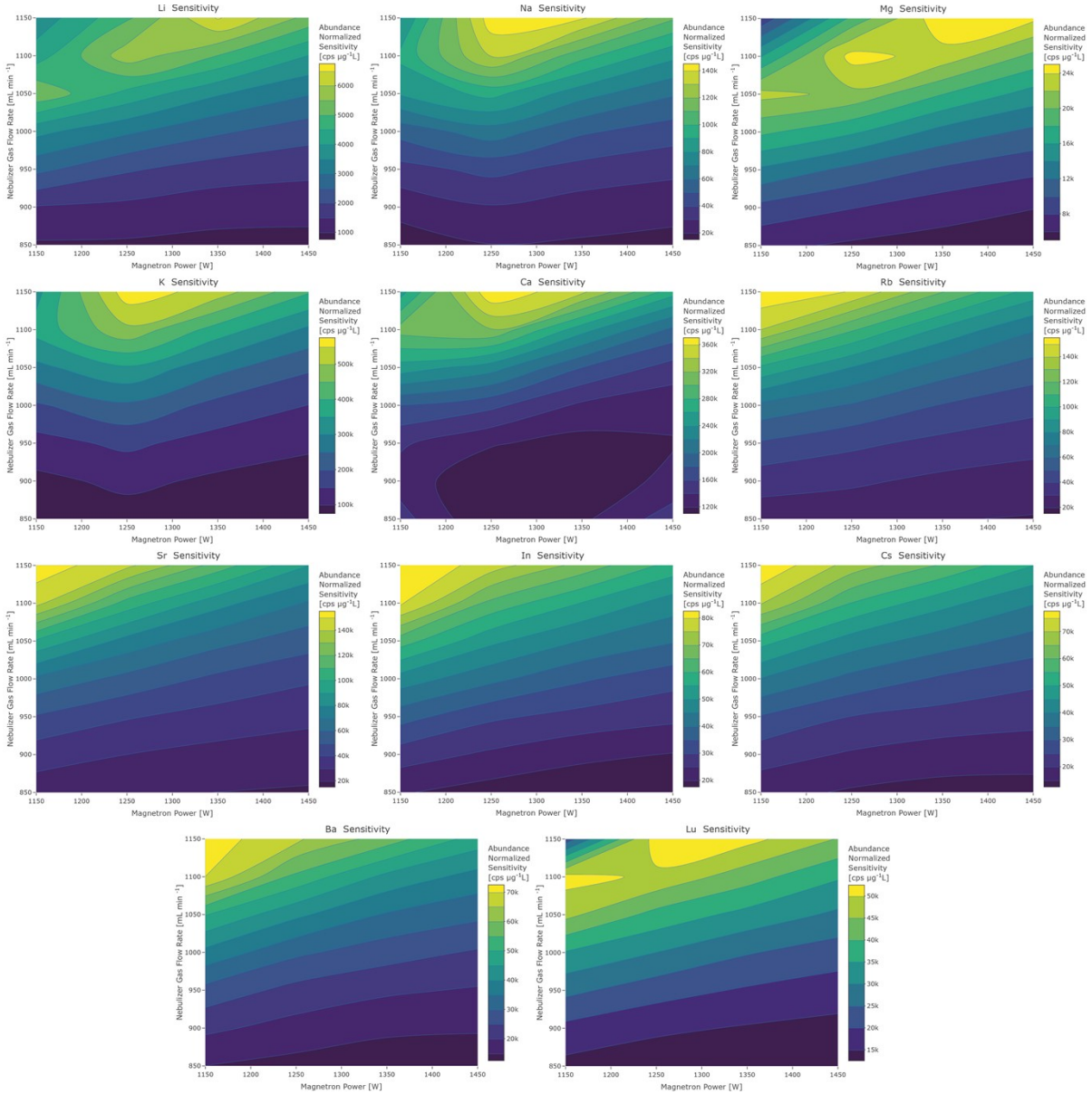

Figure S16: Sensitivity contour plots for the analytes ^{7}Li, ^{23}Na, ^{24}Mg, ^{39}K, ^{40}Ca, ^{85}Rb, ^{88}Sr, ^{115}In, ^{133}Cs, ^{137}Ba and ^{175}Lu that belong to the first group, measured with the reduced sampler. Since the bimodal behaviour of the ^{40}Ca sensitivity was not observed for this interface configuration, ^{40}Ca was not considered as a third group analyte.

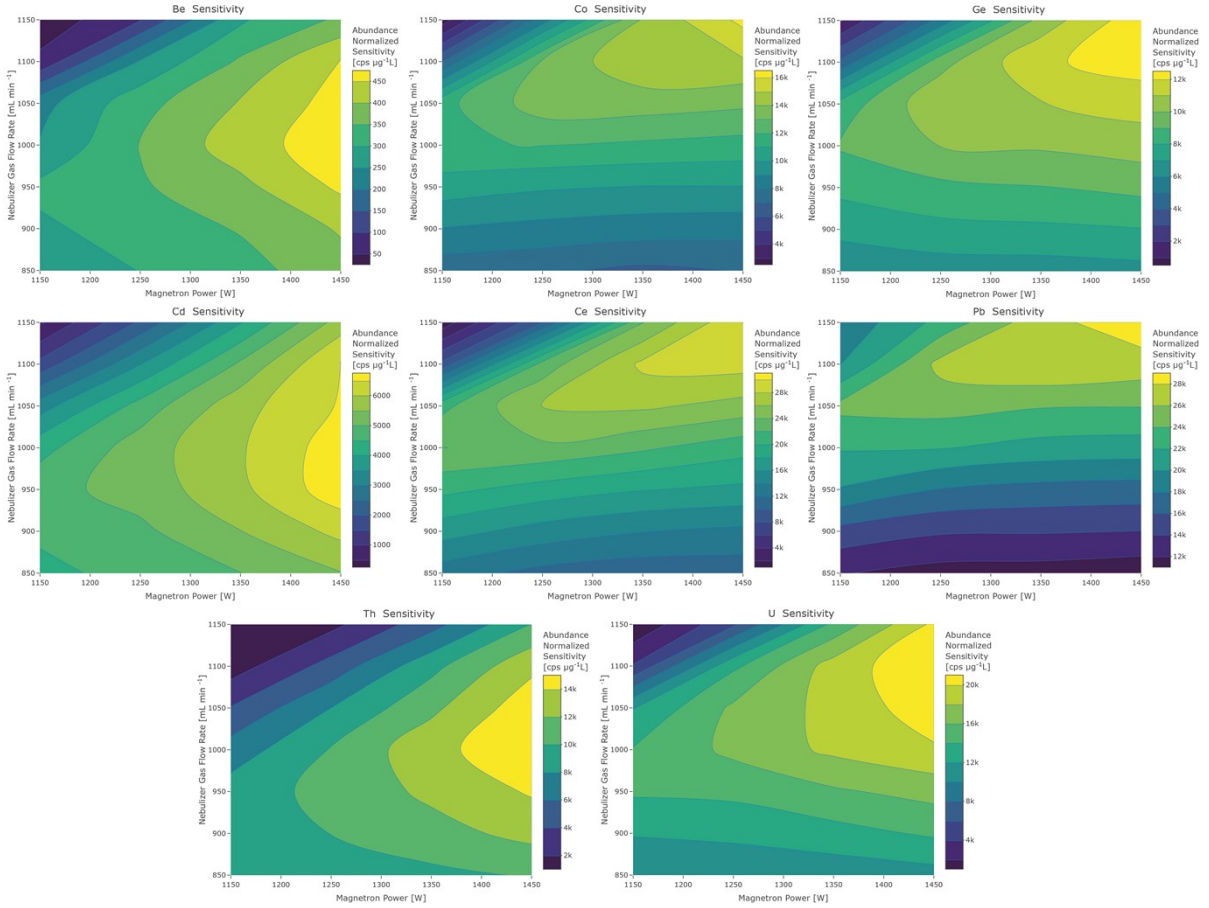

Figure S17: Sensitivity contour plots for the analytes ^{9}Be, ^{59}Co, ^{72}Ge, ^{111}Cd, ^{140}Ce, ^{208}Pb, ^{232}Th and ^{238}U that belong to the second group, measured with the reduced sampler.

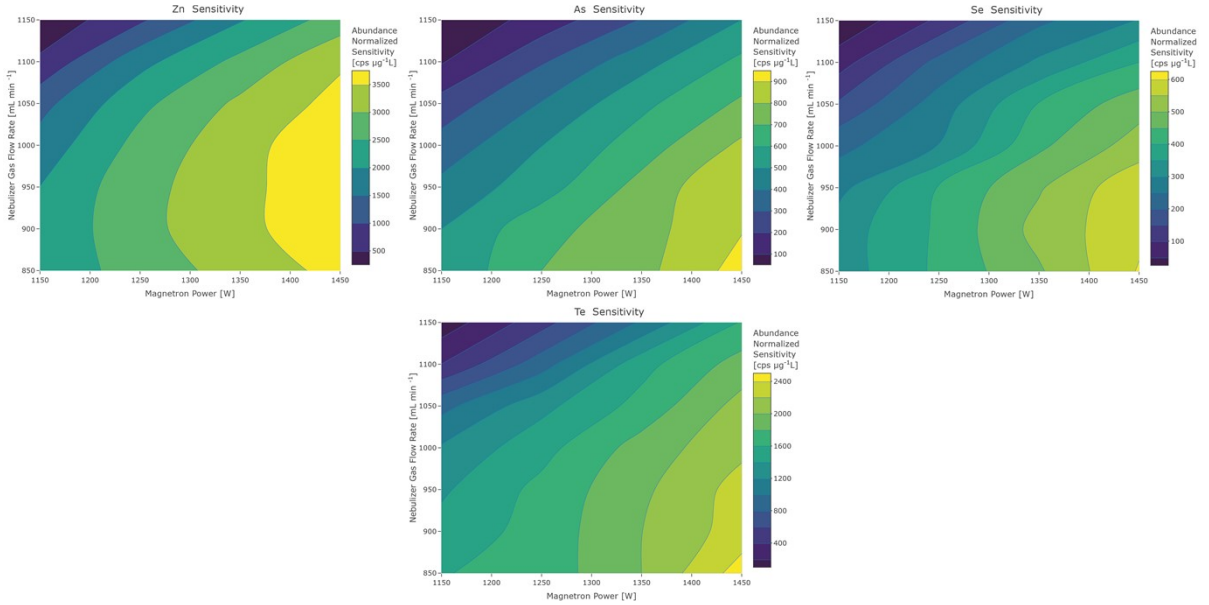

Figure S18: Sensitivity contour plots for the analytes ^{66}Zn, ^{75}As, ^{80}Se and ^{128}Te that belong to the third group, measured with the reduced sampler. Since the bimodal behaviour of ^{40}Ca sensitivity was not observed for this interface configuration, ^{40}Ca was considered a first group analyte.

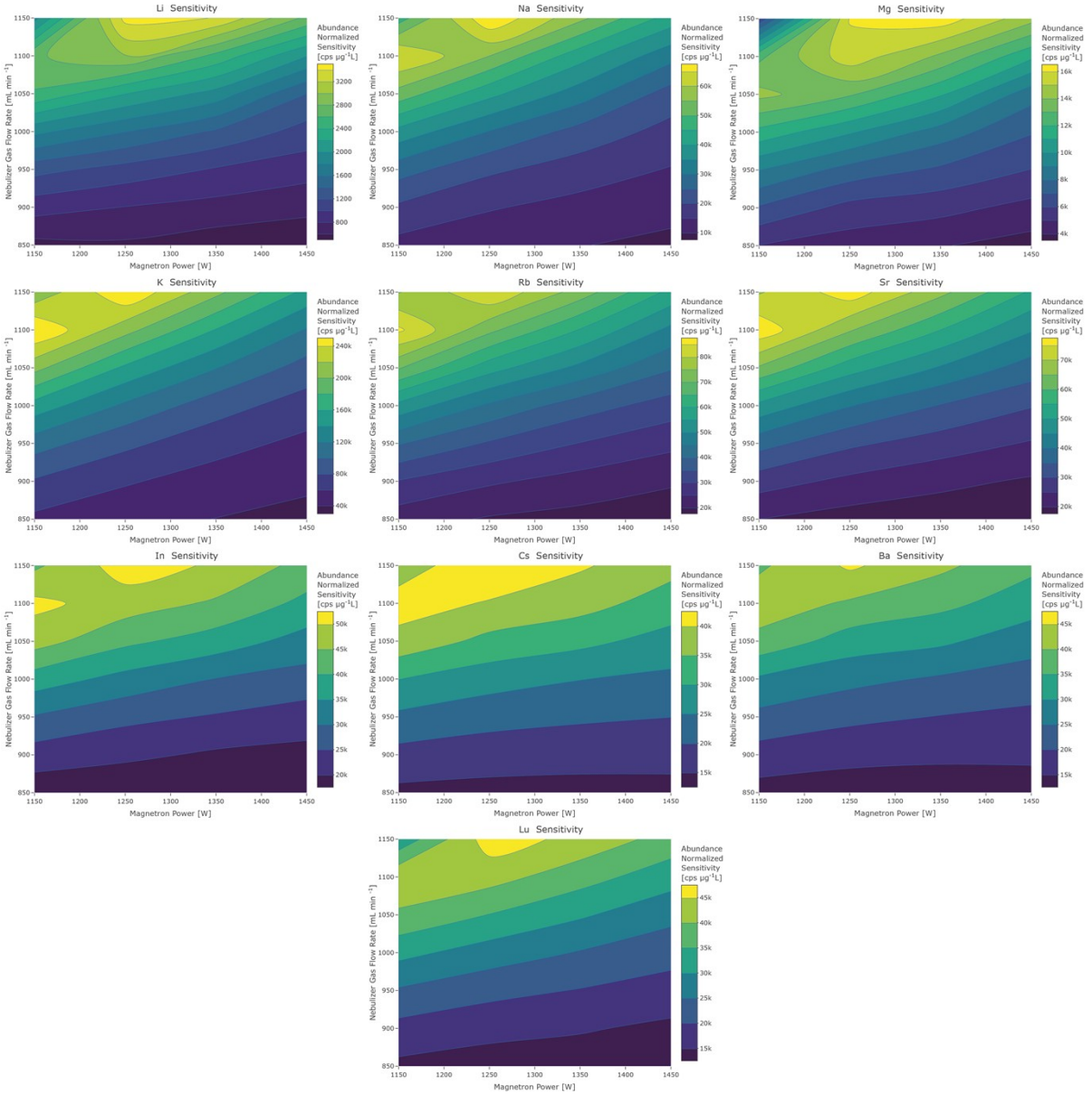

Figure S19: Sensitivity contour plots for the analytes ^{7}Li, ^{23}Na, ^{24}Mg, ^{39}K, ^{85}Rb, ^{88}Sr, ^{115}In, ^{133}Cs, ^{137}Ba and ^{175}Lu that belong to the first group, measured with the standard interface & the second interface pump.

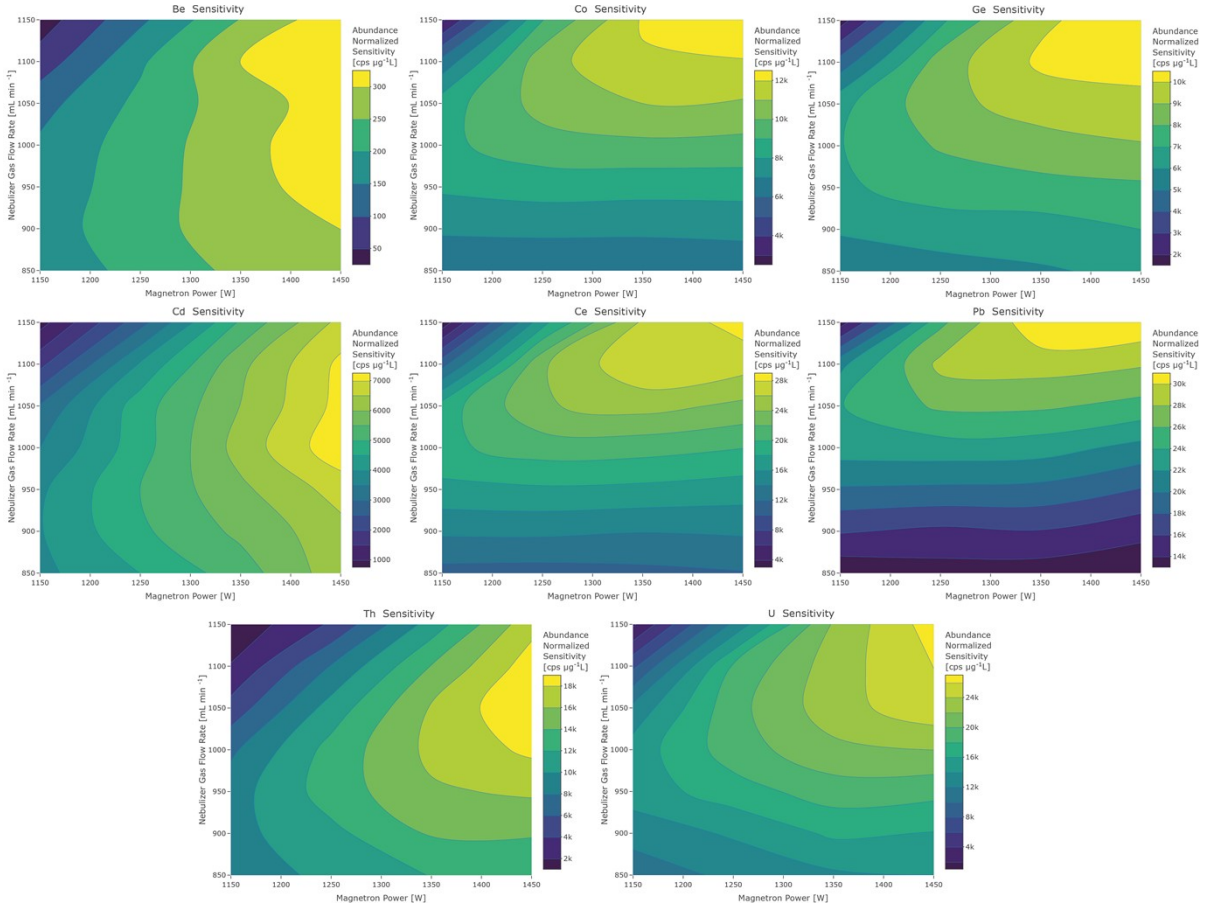

Figure S20: Sensitivity contour plots for the analytes ^{9}Be, ^{59}Co, ^{72}Ge, ^{111}Cd, ^{140}Ce, ^{208}Pb, ^{232}Th and ^{238}U that belong to the second group, measured with the standard interface & the second interface pump.

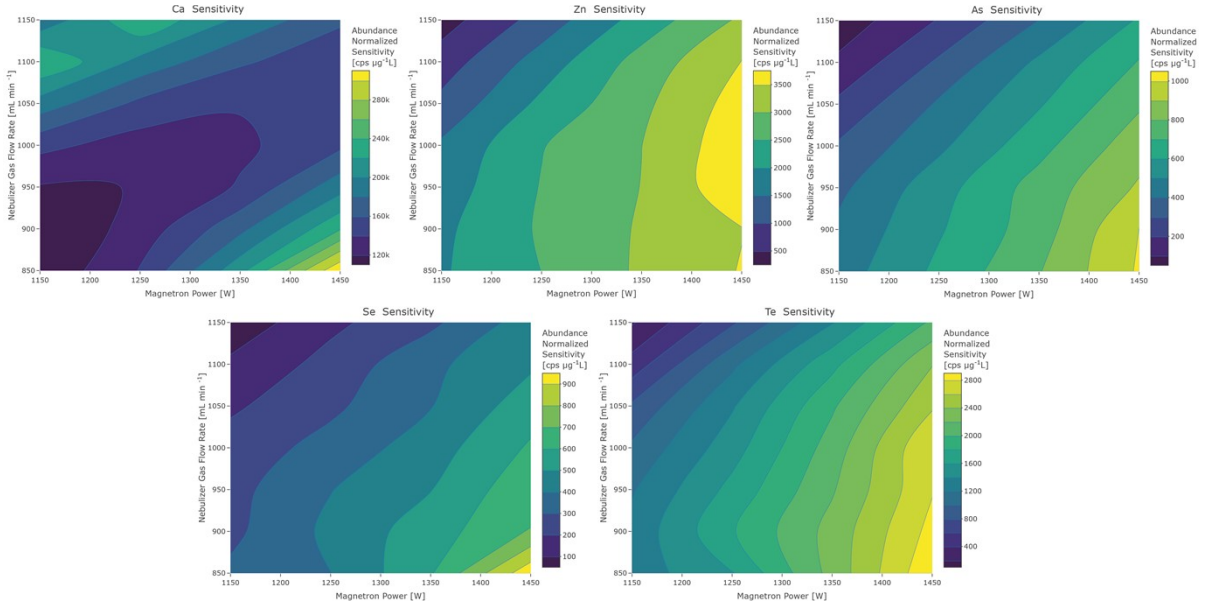

Figure S21: Sensitivity contour plots for the analytes ^{40}Ca, ^{66}Zn, ^{75}As, ^{80}Se and ^{128}Te that belong to the third group, measured with the standard interface & the second interface pump.

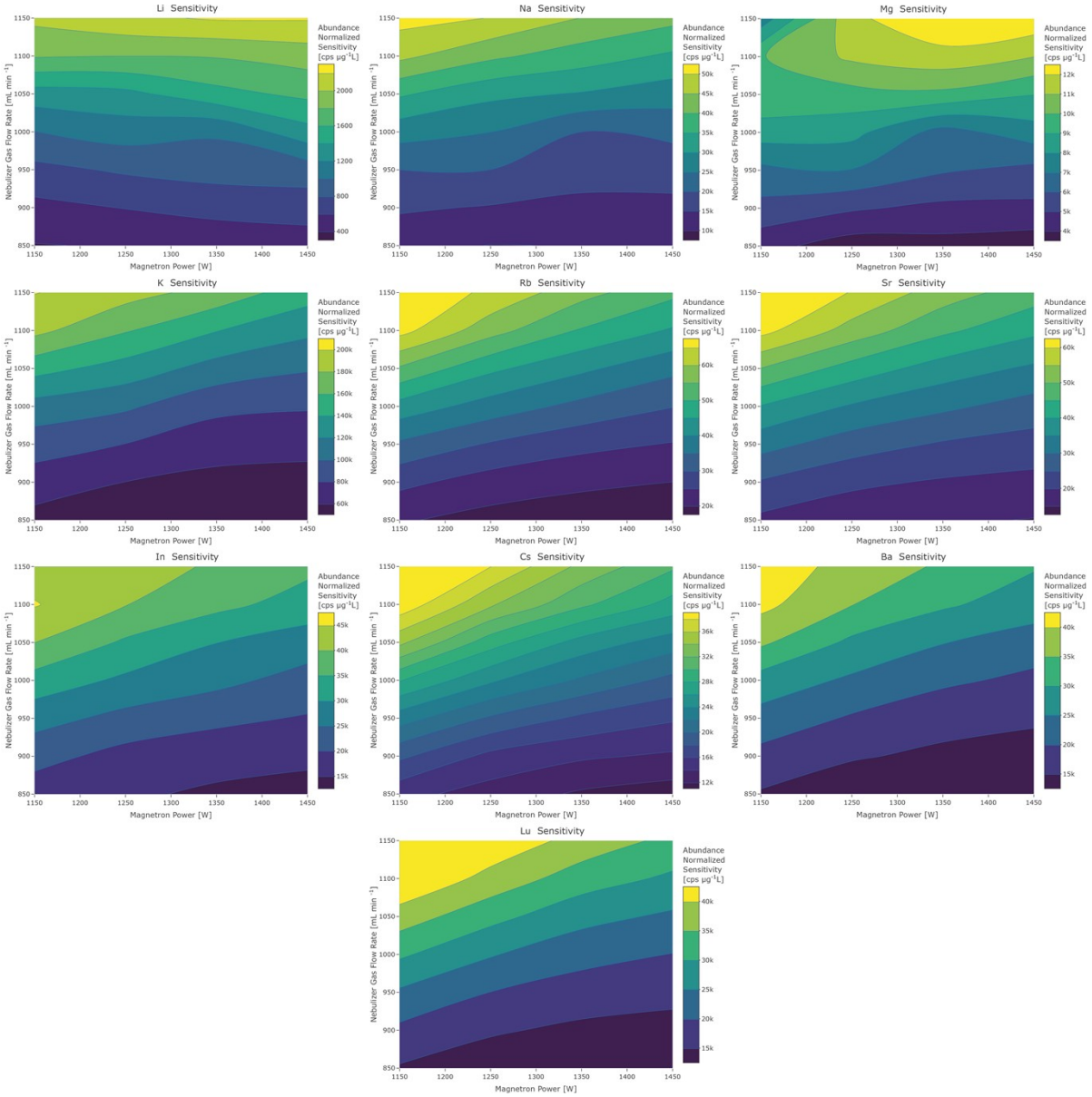

Figure S22: Sensitivity contour plots for the analytes ^{7}Li, ^{23}Na, ^{24}Mg, ^{39}K, ^{85}Rb, ^{88}Sr, ^{115}In, ^{133}Cs, ^{137}Ba and ^{175}Lu that belong to the first group, measured with 0.5 mm skimmer shift. Here, the ^{24}Mg may also be considered as an analyte of the second group.

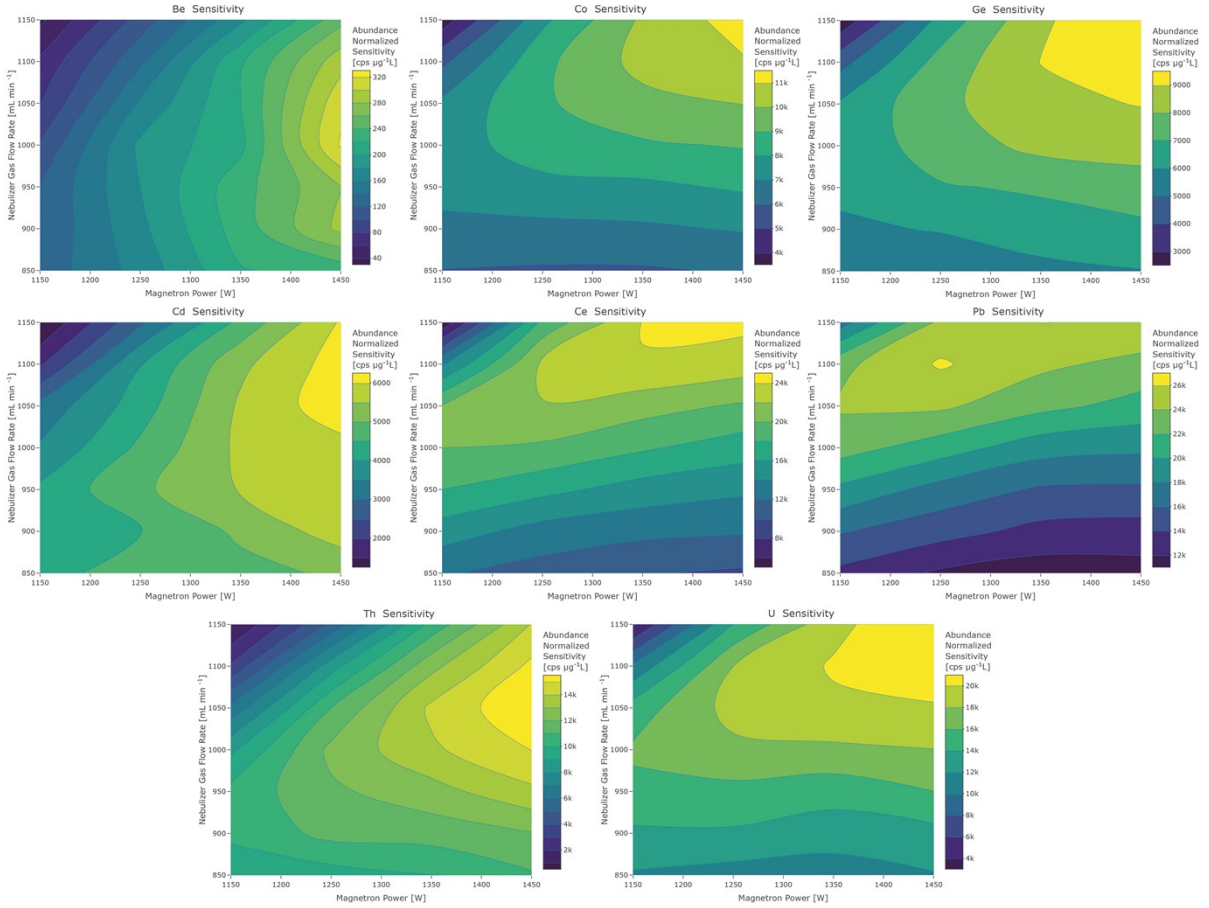

Figure S23: Sensitivity contour plots for the analytes ^{9}Be, ^{59}Co, ^{72}Ge, ^{111}Cd, ^{140}Ce, ^{208}Pb, ^{232}Th and ^{238}U that belong to the second group, measured with a 0.5 mm skimmer shift.

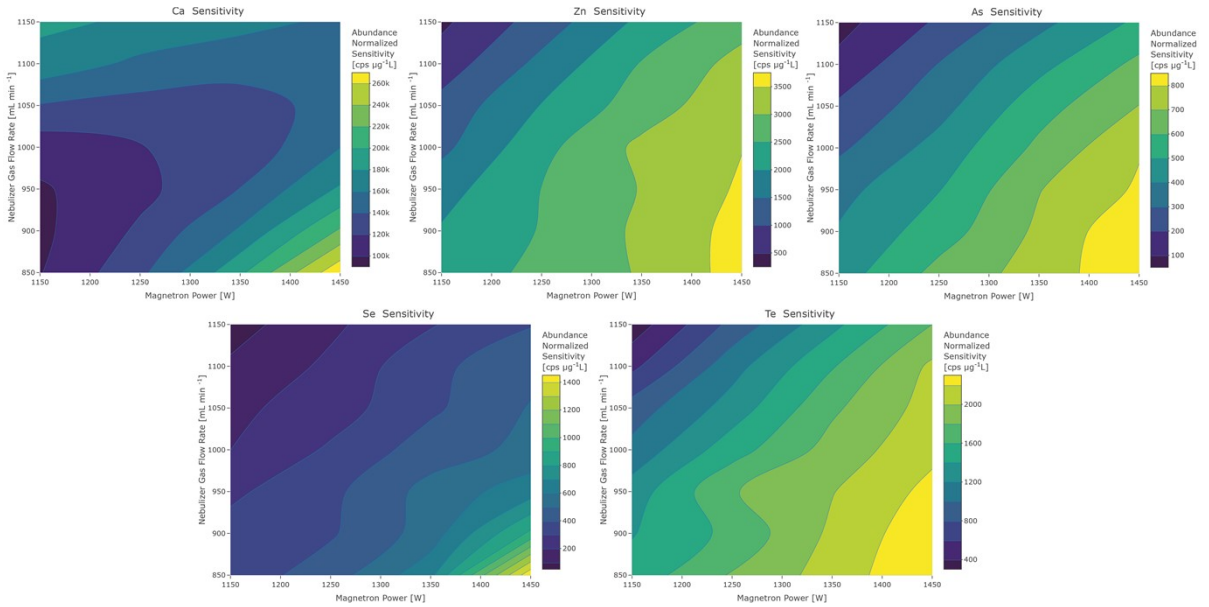

Figure S24: Sensitivity contour plots for the analytes ^{40}Ca, ^{66}Zn, ^{75}As, ^{80}Se and ^{128}Te that belong to the third group, measured with a 0.5 mm skimmer shift.

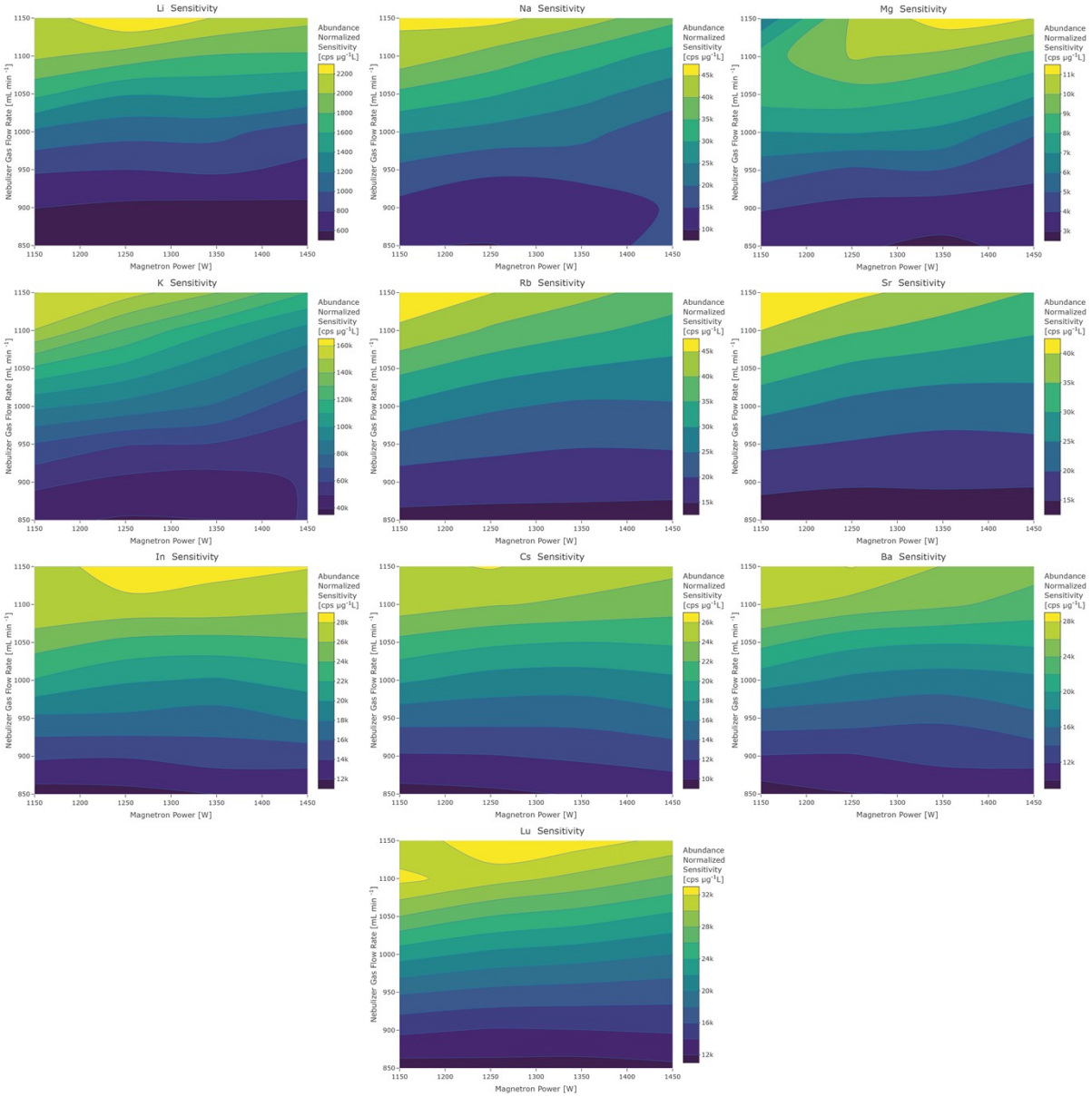

Figure S25: Sensitivity contour plots for the analytes ^{7}Li, ^{23}Na, ^{24}Mg, ^{39}K, ^{85}Rb, ^{88}Sr, ^{115}In, ^{133}Cs, ^{137}Ba and ^{175}Lu that belong to the first group, measured with 1.0 mm skimmer shift.

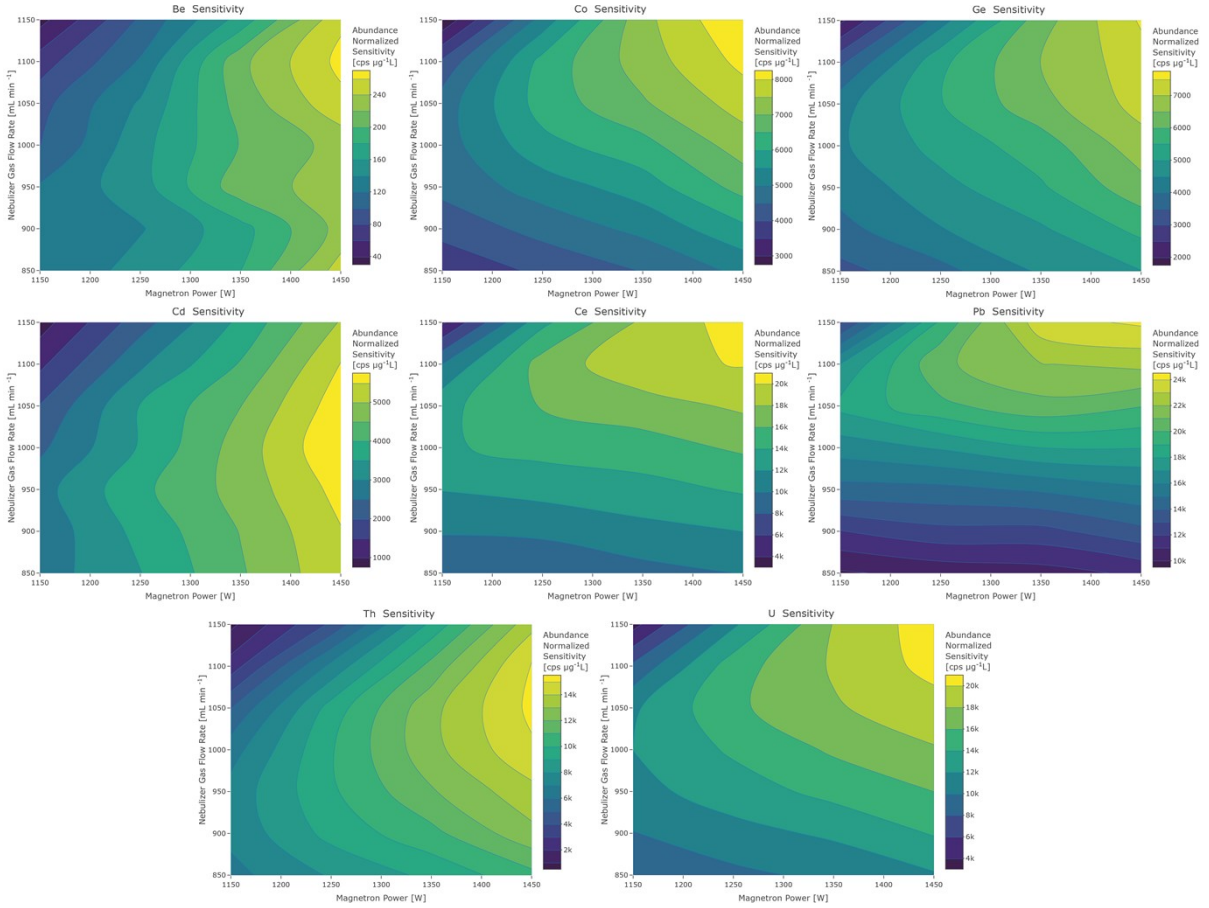

Figure S26: Sensitivity contour plots for the analytes ^{9}Be, ^{59}Co, ^{72}Ge, ^{111}Cd, ^{140}Ce, ^{208}Pb, ^{232}Th and ^{238}U that belong to the second group, measured with a 1.0 mm skimmer shift.

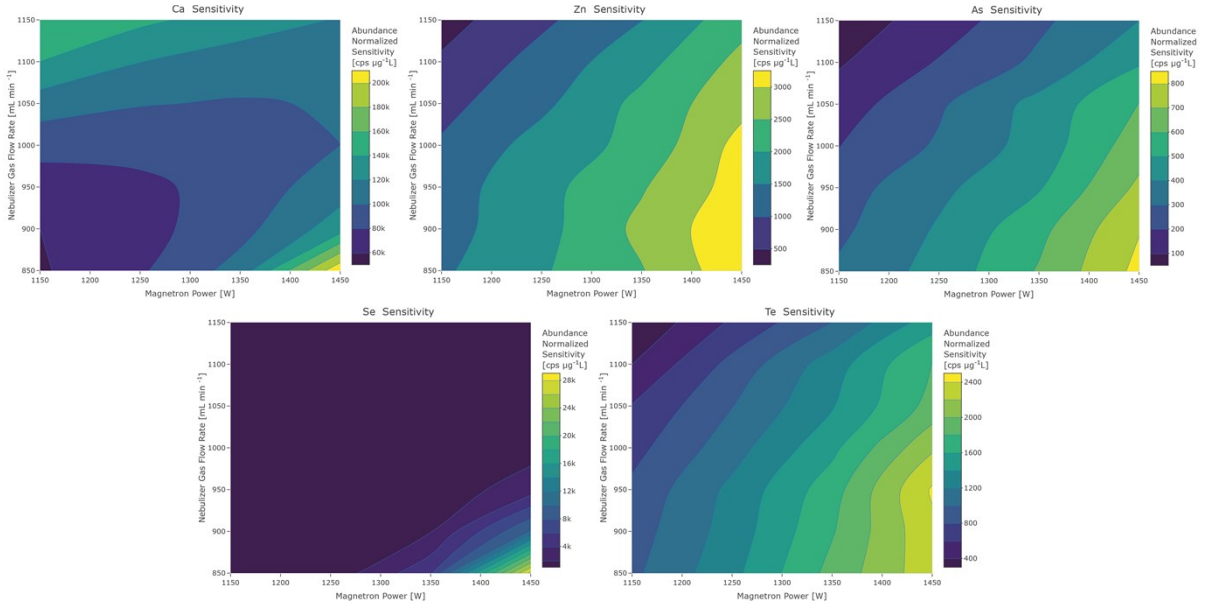

Figure S27: Sensitivity contour plots for the analytes ^{40}Ca, ^{66}Zn, ^{75}As, ^{80}Se and ^{128}Te that belong to the third group, measured with a 1.0 mm skimmer shift. In this configuration, the behaviour of the ^{80}Se sensitivity is altered by the spectral interference.

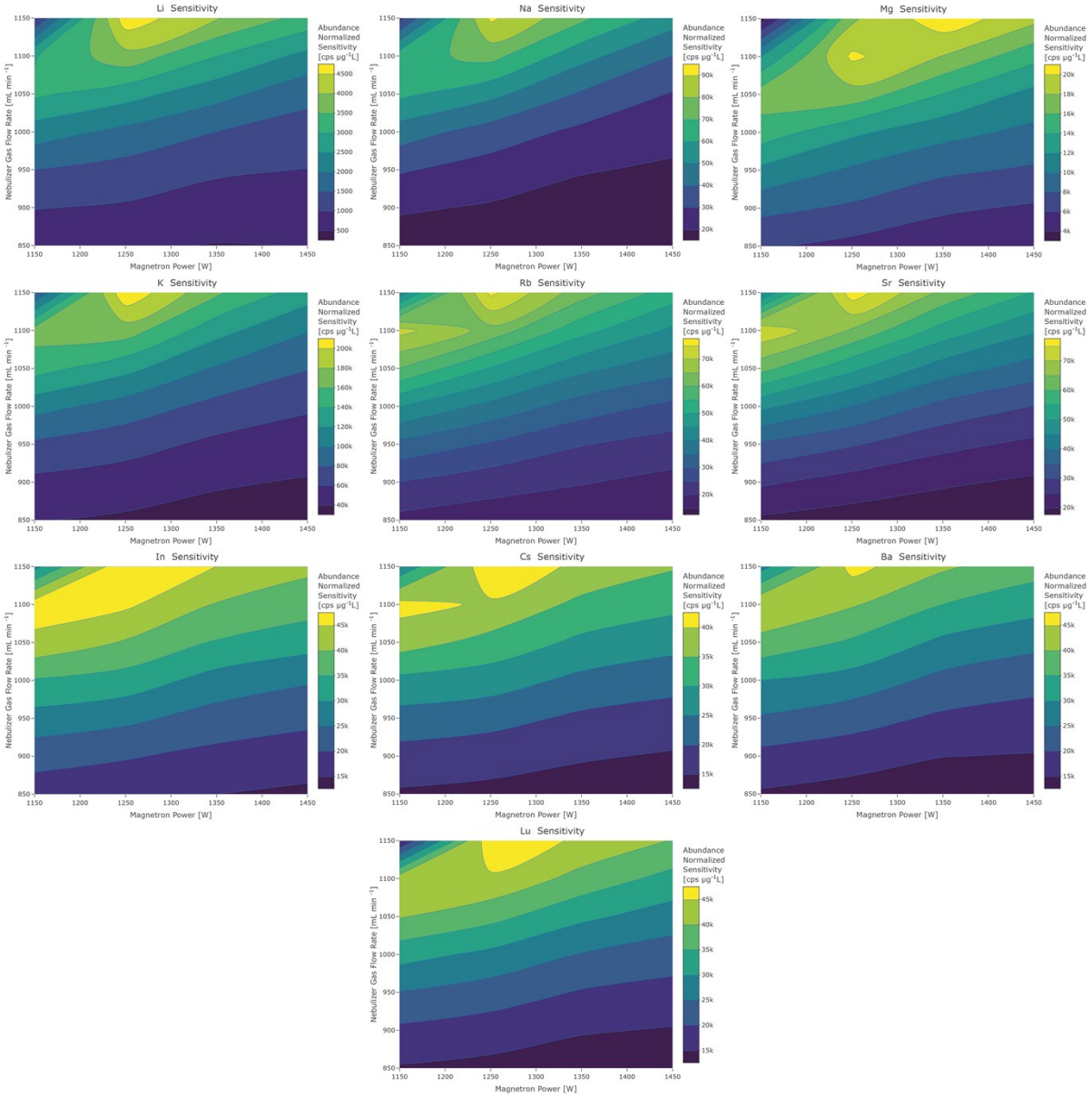

Figure S28: Sensitivity contour plots for the analytes ^{7}Li, ^{23}Na, ^{24}Mg, ^{39}K, ^{85}Rb, ^{88}Sr, ^{115}In, ^{133}Cs, ^{137}Ba and ^{175}Lu that belong to the first group, measured with 0.5 mm skimmer shift & the second interface pump.

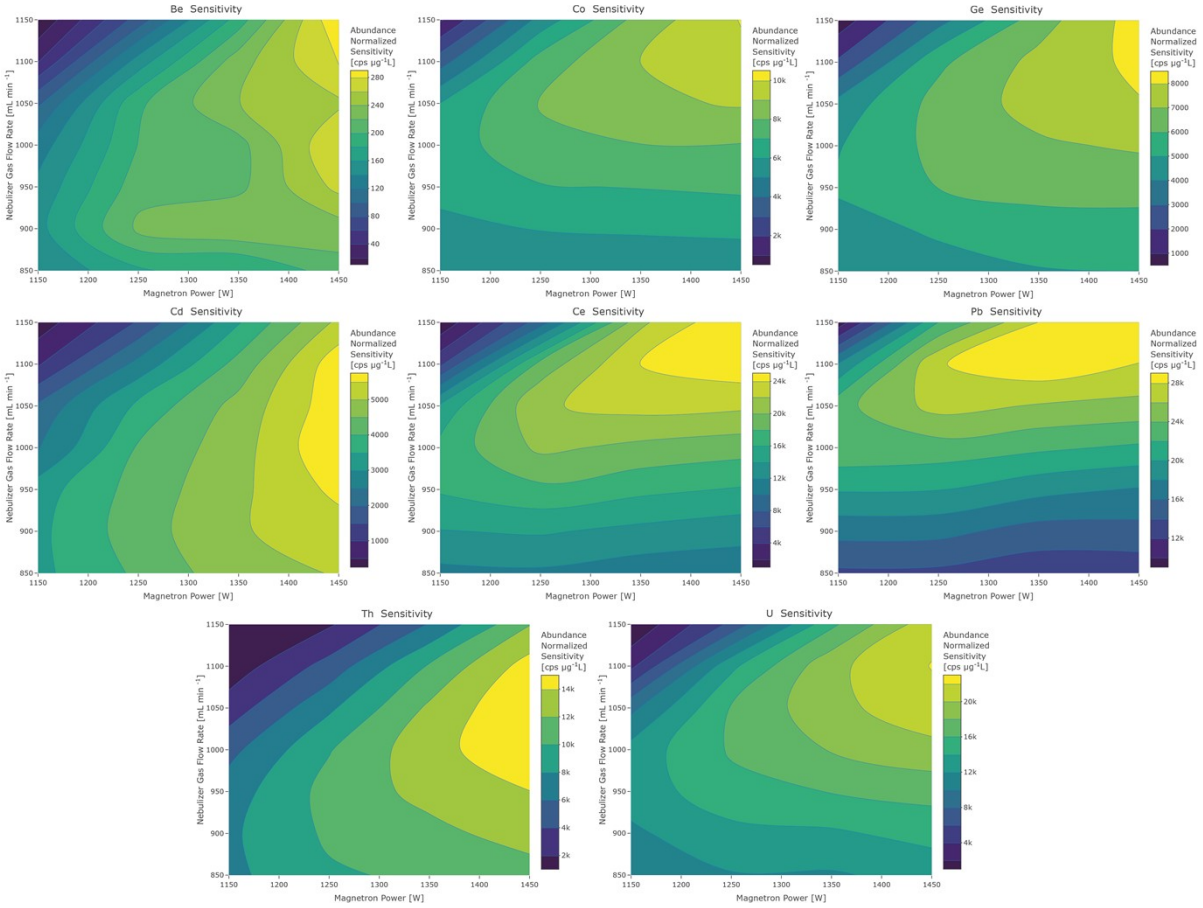

Figure S29: Sensitivity contour plots for the analytes ^{9}Be, ^{59}Co, ^{72}Ge, ^{111}Cd, ^{140}Ce, ^{208}Pb, ^{232}Th and ^{238}U that belong to the second group, measured with a 0.5 mm skimmer shift & the second interface pump.

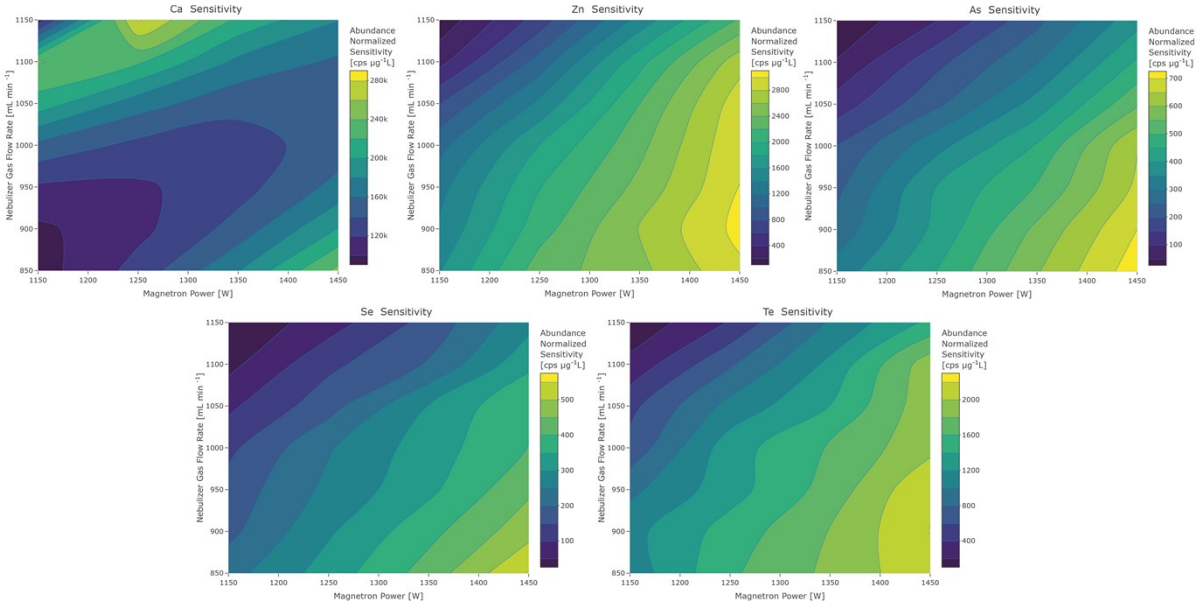

Figure S30: Sensitivity contour plots for the analytes ^{40}Ca, ^{66}Zn, ^{75}As, ^{80}Se and ^{128}Te that belong to the third group, measured with a 0.5 mm skimmer shift & the second interface pump.

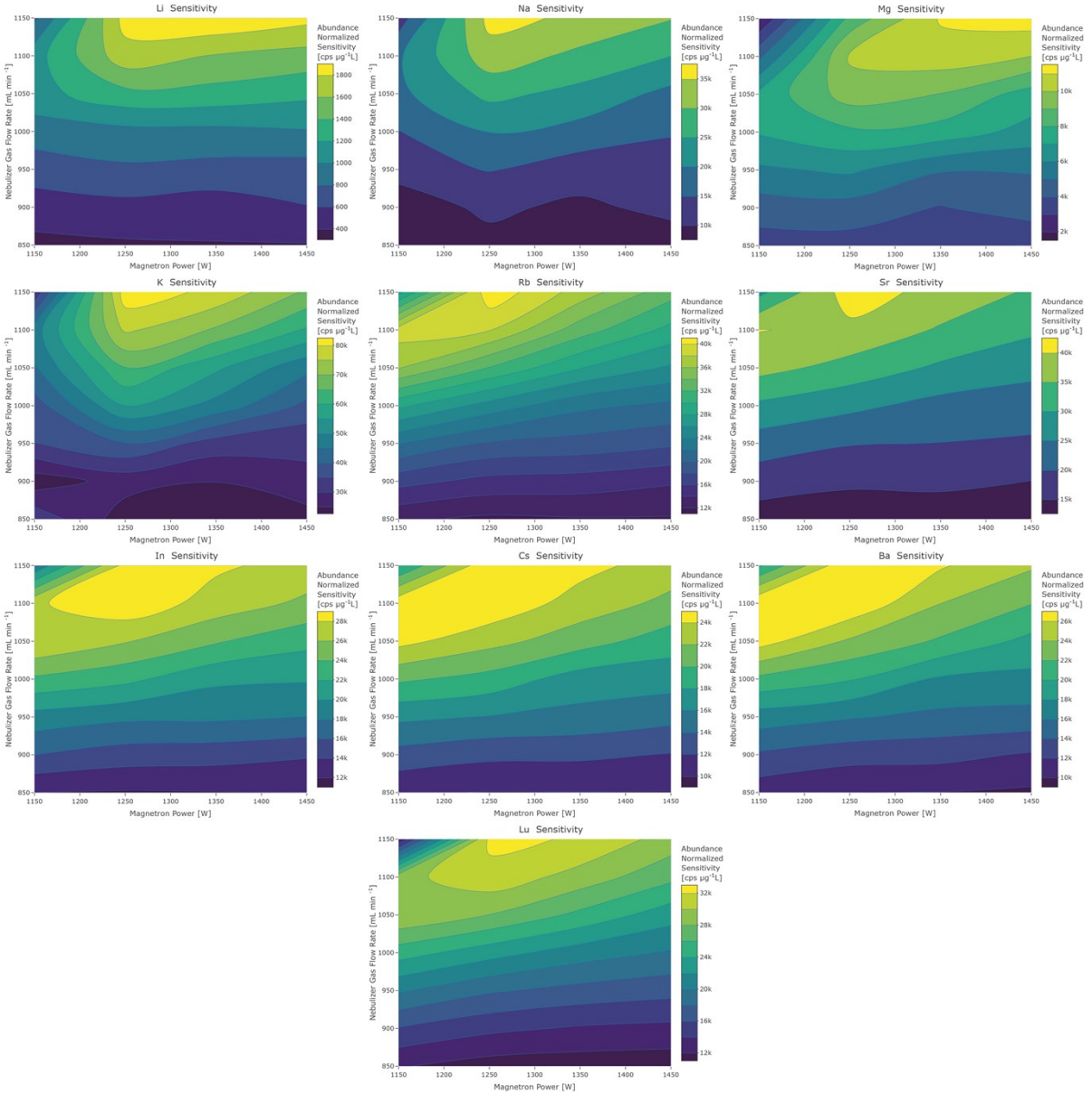

Figure S31: Sensitivity contour plots for the analytes ^{7}Li, ^{23}Na, ^{24}Mg, ^{39}K, ^{85}Rb, ^{88}Sr, ^{115}In, ^{133}Cs, ^{137}Ba and ^{175}Lu that belong to the first group, measured with 1.0 mm skimmer shift & the second interface pump.

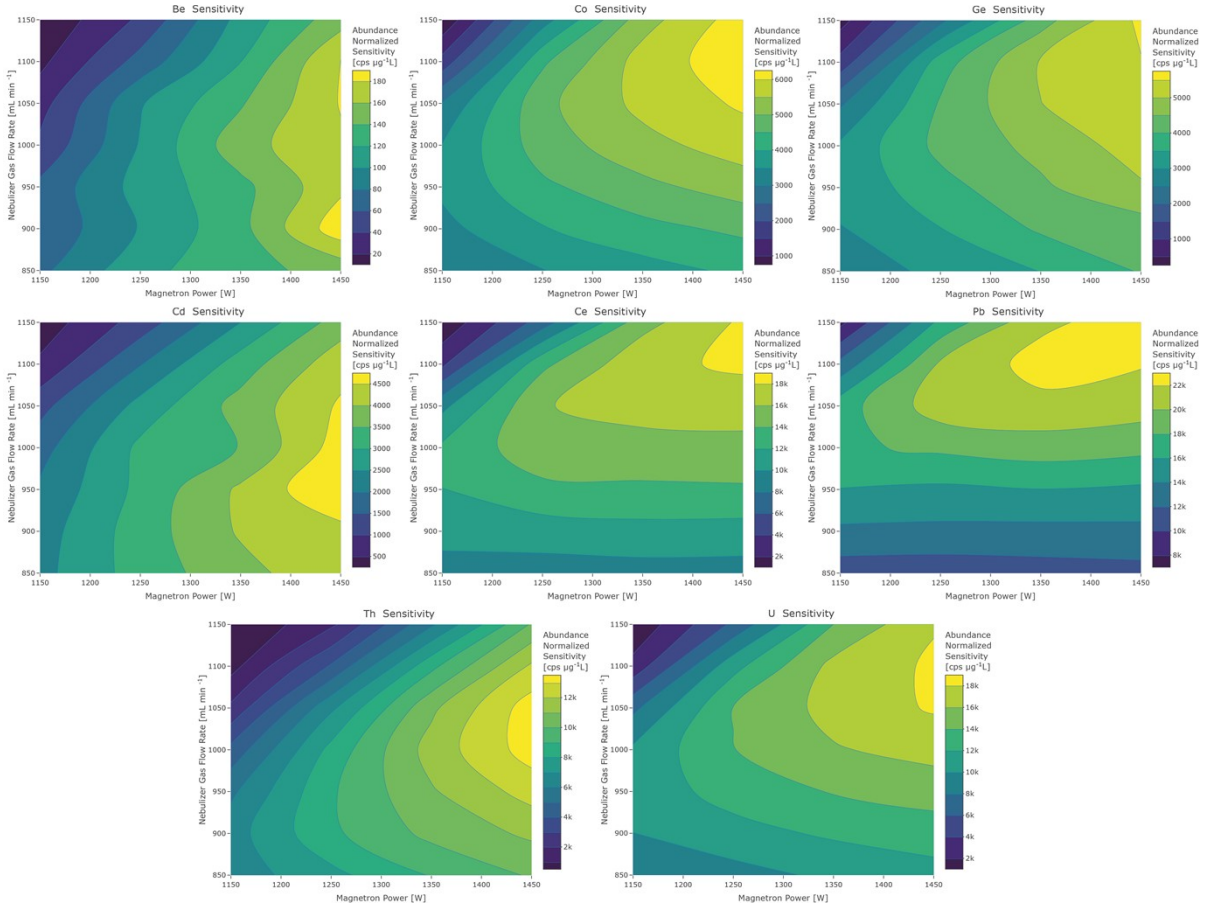

Figure S32: Sensitivity contour plots for the analytes ^{9}Be, ^{59}Co, ^{72}Ge, ^{111}Cd, ^{140}Ce, ^{208}Pb, ^{232}Th and ^{238}U that belong to the second group, measured with a 1.0 mm skimmer shift & the second interface pump.

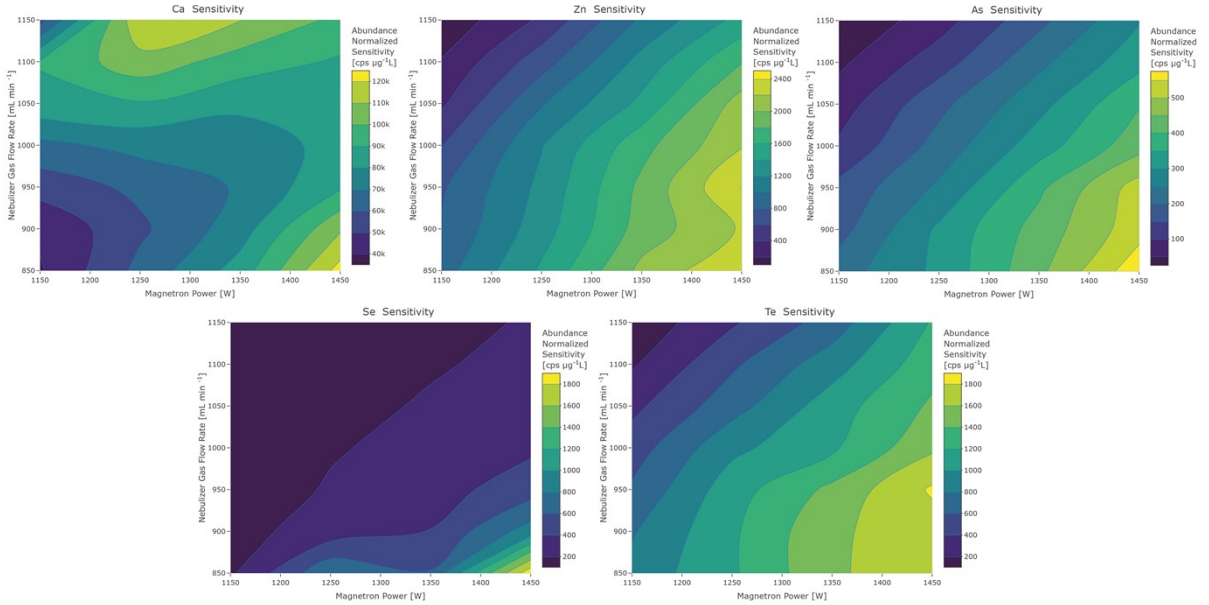

Figure S33: Sensitivity contour plots for the analytes ^{40}Ca, ^{66}Zn, ^{75}As, ^{80}Se and ^{128}Te that belong to the third group, measured with a 1.0 mm skimmer shift & the second interface pump. In this configuration, the behaviour of the ^{80}Se sensitivity is altered by the spectral interference.

Table S1: An overview of the N_2 MICAP MS operating conditions employed during this study. The ion lens voltage has been re-

Parameter	Value
Cooling Gas Flow Rate	14 L min^{-1}
Auxiliary Gas Flow Rate	750 mL min^{-1}
Nebulizer Gas Flow Rate[a]	800 – 1100 mL min^{-1}
Magnetron Power[a]	1150 – 1450 W
Ion Lens	variable
Quadrupole Rod Offset [Standard Mode]	-5 V
Cell Rod Offset [Standard Mode]	-15 V
Cell Path Voltage [Standard Mode]	-50 V

calibrated after each change of interface configuration or operating parameter.

[a] were varied in steps of 50 mL min^{-1} respectively 100 W

Table S2: Detection limits for the N_2-MICAP are given in ng mL^{-1} with the corresponding blank signal and its standard deviation.

Element	Isotope	Blank Signal [cps]	Standard Deviation [cps]	Sensitivity [cps / ng mL^{-1}]	Limits of Detection [ng mL^{-1}]
Li	7	80	14	1’400	0.03
Be	9	18	4	300	0.04
B	11	140	22	440	0.15
Mg	24	160	20	30’000	0.002
Ca	40	56’000	400	25’000	0.05
V	51	40	6	16’000	0.001
Cr	52	30	8	14’000	0.001
Mn	55	18	8	18’000	0.001
Fe	56	4’800	70	12’000	0.017
Fe	57	90	11	350	0.09
Co	59	30	6	8’000	0.002
Ni	60	86	20	3’000	0.02
Zn	66	50	5	1’700	0.009
Ga	69	30	7	10’000	0.002
Ga	71	8	4	7’000	0.002
As	75	10	5	1’100	0.012
Se	78	8	4	160	0.07
Se	80	30	9	330	0.08
Rb	85	19	9	20’000	0.001
Sr	88	30	11	20’000	0.002
Mo	95	12	5	3’000	0.006
Mo	98	7	3	4’000	0.002
Ag	107	14	6	6’000	0.003
Cd	111	6	5	1’000	0.017
Te	128	6	4	1’200	0.009
Ba	137	9	3	3’000	0.003
Ba	138	18	8	20’000	0.001
Pb	208	9	4	12’000	0.001
Bi	209	7	3	14’000	0.0007
U	238	8	3	30’000	0.0003

The sensitivity was calculated from a diluted Certipur® ICP multi-element standard solution VI from Merck.